Inferential MIMO predictive control of the particle size distribution in emulsion polymerization

Bruno da Silva, Pascal Dufour, Nida Sheibat-Othman, Sami Othman

1
Université de Lyon, Lyon, F-69003, France; Université Lyon 1;
CNRS UMR 5007 LAGEP (Laboratoire d'Automatique et de GEnie des Procédés),
43 bd du 11 novembre, 69100 Villeurbanne, France
Tel +33 (0) 4 72 43 18 45 - Fax +33 (0) 4 72 43 16 99
http://www-lagep.univ-lyon1.fr/ http://www.univ-lyon1.fr http://www.cnrs.fr

Inferential MIMO predictive control of the particle size distribution in emulsion polymerization

Bruno da Silva, Pascal Dufour*, Nida Sheibat-Othman, Sami Othman

Université de Lyon, F-69622, France;

Université Lyon 1, Villeurbanne;

CNRS, UMR 5007, LAGEP;

43 bd du 11 novembre, 69622 Villeurbanne Cedex, France

* Corresponding author, e-mail: dufour@lagep.univ-lyon1.fr, phone: +33 4 72 43 18 78,

fax: +33 4 72 43 16 99, http://www.tinyurl.com/dufourpascal

Abstract

A new inferential 2-step multiple input/multiple output (MIMO) model predictive control (MPC) of the particle size distribution (PSD) in emulsion polymerization processes is proposed. The bulk-like model describing the PSD is used with the material balances of initiator, radicals, monomer and surfactant. The inferential 2-step control strategy uses two measurements available online (without delay): the concentration of surfactant in the aqueous phase by conductimetry, and the concentration of monomer by calorimetry. In a first step, the optimal trajectory of surfactant concentration leading to the target PSD is calculated offline. In a second step, a multivariable model predictive control manipulates online the monomer and surfactant flow rates in order to track the precalculated surfactant concentration trajectory and to maximize the monomer concentration in the polymer particles in a constrained set-point tracking. Two control strategies are compared (nonlinear MPC and linearized MPC) with and without modelling errors.

Keywords

Model predictive control ; emulsion polymerization ; particle size distribution ; nonlinear distributed parameter system ; inferential control.

1 Introduction

Polymers are the bases of many products. A big part of these products is produced by emulsion polymerization, such as dispersions (paints and adhesives, such as polyvinyl acetate, acrylic polymers), plastics after particle coagulation (e.g.: polystyrene, polymethyl methacrylate) and rubber (e.g.: styrene butadiene rubber, neoprene rubber). This process has several advantages over other free radical polymerization processes comprising the high conversion rate (close to 100%) and the low viscosity of the medium which enhances temperature control and reaction mixing. Also, the continuous phase in this process is water which reduces the amount of volatile organic compounds. The emulsion medium contains the monomer (usually water insoluble) which is the basis of the polymer, the reaction initiator and the surfactant which allows stabilization of the monomer droplets and polymer particles. The latex produced by emulsion polymerization is characterized by its polymer molecular weight and particle size distribution (PSD). The molecular weight distribution affects the mechanical properties of the final polymer, whereas the PSD affects the rheological and optical properties of the latex and its stability. The PSD also affects film formation properties of the latex (Geurts et al., 1996). Berend and Richtering (1995) studied the rheology of monodispersed and bidispersed lattices and concluded that the viscosity depends on the volume fraction of small to big particles and on the size of each population (see figure 1). Schneider et al. (2002) have shown that bimodal PSD allows increasing the solid content while maintaining a low viscosity (compared to monomodal PSD), which is of interest since high solid contents are usually desired in order to reduce transport costs and drying time. Therefore, it appears that

controlling the PSD (of the final latex) is primordial to obtain specific end-use properties for paints and adhesives.

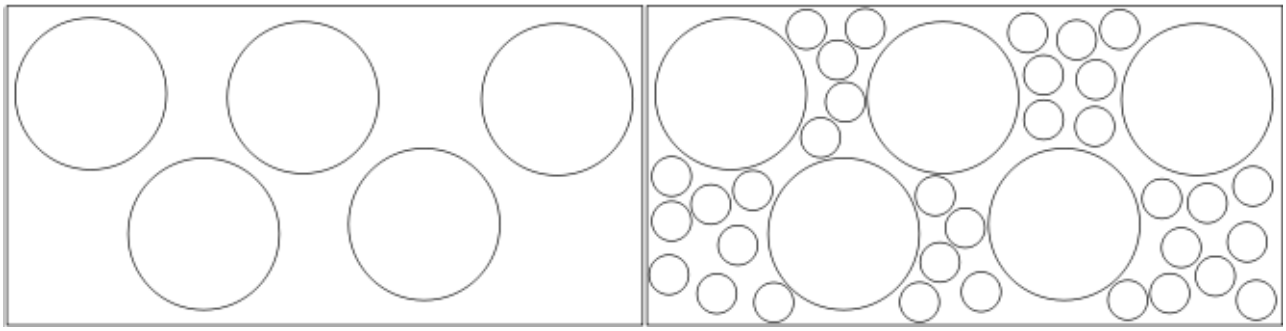

Figure 1 - Monomodal PSD latex particles (left) and bimodal PSD latex particles (right).

It is worthy to note that the process model describing the PSD is nonlinear, distributed and includes an important number of parameters that are not well known or sensitive to impurities. This renders the model-based control of the PSD a difficult task. Moreover, online measurement of bimodal PSD is not available. Existing technologies (such as light scattering) mainly concern the measurement of monodispersed lattices and operate offline. Elizalde et al. (2000) and Schneider and McKenna (2002) realised a comparative study of technologies used to measure the PSD. Separative technologies, such as capillary hydrodynamic fractionation (CHDF), were found to be the most adapted for multi-dispersed lattices. But, the main inconvenience of these techniques is the long analysis time. Therefore, these measurements can hardly be used in an online closed-loop control scheme. An interesting alternative measurement for controlling the PSD is the online measurement of the concentration of free surfactant in the aqueous phase which gives information about the stability of particles and the concentration of micelles. Santos et al. (2007) used the conductimetry and ion-selective electrodes to measure the concentration of free anionic surfactant molecules (sodium dodecyl sulfate) in the aqueous phase in emulsion polymerisation.

Until now, the control of the PSD was treated in different ways in the literature to obtain a bimodal PSD. For the PSD control in such processes, one may distinguish, batch to batch, indirect and direct control strategies (Kiparissides, 2006):

- Batch to batch control

In this method, an offline optimization study is first realised based on the process model to determine the optimal input profiles that give the desired PSD. Then, the obtained input profiles are applied experimentally, therefore assuming perfect process modelling. By collecting measurements after each batch, modelling errors can be corrected and can be assumed to remain unchanged for a given lot of products. By applying this method, Crowley et al. (2000) used the surfactant flow rate to control the PSD. The so-called zero-one model was used to represent the PSD in a semi-batch emulsion polymerization of styrene. Flores-Cerillo and MacGregor (2002) proposed a batch to batch control strategy by adding an online correction of the surfactant concentration in the middle of the reaction using a prediction of the PSD obtained by partial least square models (based on online temperature measurements and offline surface tension and PSD measurements). Immanuel and Doyle III (2002) used an open loop genetic control algorithm to predict the control profiles to obtain the desired PSD of a copolymerization process. Doyle III et al. (2003) proposed a hybrid model-based approach for batch-to-batch control of the PSD. A fundamental population balance model describing the PSD evolution was augmented by a partial least squares model. By this way, only slight batch-to-batch correction was required. Both the surfactant and initiator flow rates were manipulated. Online measurement of the full PSD was assumed available, which is still a challenging issue. The batch to batch iterative feedback PSD control was also used by Immanuel et al. (2008). They considered correction of modelling errors from batch to batch. Recently, Alamir et al. (2010) applied an iterative learning control of the PSD by proposing a simplified behavioural model to describe the PSD. Besides offline correction of the model and

control inputs, delayed online measurements of the PSD were used in the feedback control. Using a behavioural model represents an advantage due to its simplicity and therefore shorter run time, even though it might increase the batch to batch correction level.

- Indirect (or inferential) control

In inferential control, even though the desired property to control is not measured online, the controller uses the available measurements to fulfil its objective. Abedini and Shahrokhi (2008) used the measurement of the surfactant concentration to control the PSD by a single input/single output PID controller that tunes the free surfactant flow rate. They assumed 5% impurities in the surfactant and 10% model mismatch mainly in the coefficient of propagation rate and the diffusion coefficient of monomer, to evaluate the robustness of their strategy. The monomer concentration was not controlled.

- Direct control

Closed-loop direct control corresponds to the control of the PSD using its online measurement or an estimate that can be based on its discontinuous measurement. It appears that in the case of PSD control, direct control can only be based on an estimate of the PSD since there is a delay in its measurement. Alhamad et al. (2005) and Zeaiter et al. (2006) used MPC to broaden the PSD. Real outputs were inferred by open-loop model simulation combined with a corrective term of the model using CHDF offline delayed measurements. Alhamad et al. (2005) manipulated the flow rates of the monomers (styrene and methyl methacrylate), surfactant and initiator and used the zero-one kinetic model. Zeaiter et al. (2006) manipulated only the monomer flow rate (styrene) and used a model generated through linearization around the offline optimal trajectory. Therefore, the authors did not manipulate the surfactant flow rate, which is however known to be the main control variable of the PSD. Moreover, in no continuous online measurements were available for the closed loop control, even not the monomer conversion which requires the use of a precise process model: therefore, the

robustness of such control approach is questionable, especially since the polymerization reactions are usually irreproducible and sensitive to impurities. Dokucu et al. (2008) and Dokucu and Doyle III (2008) developed different control laws to control the PSD in a semi-batch emulsion copolymerization reactor. They compared the PID and the nonlinear predictive control using quadratic dynamic matrix controller. They used two measurements: the solid content (available every minute) and the PSD (available every 12 minutes). The delay of measurement was compensated by an extended Kalman filter. In (Dokucu and Doyle III, 2008), the dynamics of the PSD were represented by a reduced order model. They used the 10 first moments of the PSD as control outputs. The linear prediction model was obtained from a nonlinear model using the step response. The use of a linear model helped to describe the variation from nominal trajectories. Dokucu et al. (2008) used principal component analysis to obtain the reduced model.

For processes explicitly described by partial differential equations (PDE) model, the controller can be implemented in two ways. The first way consists of keeping the infinite dimensional representation of the PDE model, synthesizing an infinite dimensional controller, and using a finite approximation of this controller. However, in control theory, due to the complexity of the problem, relatively few studies have been devoted to the control of processes explicitly described by PDE models, especially in the nonlinear case. The second more frequent way is therefore to construct a finite approximation of the model and then to synthesize a finite dimensional controller. The original PDE model is usually simplified into an ordinary differential equation (ODE) model using one of the following numerical methods: finite differences method, finite volume method, orthogonal collocation method, Galerkin's method, or modal decomposition. However, even if various finite dimensional methods are proposed to control such distributed parameter systems, there is no general framework yet.

In the present work, the objective is to control together the concentration of free surfactant and the concentration of monomer, which helps to get the prescribed target PSD. Indeed, Semino and Ray (1995) studied the theoretical controllability of the population balance equations of this system. They concluded that the surfactant concentration is the main control variable of the number of particles and therefore the PSD in the emulsion polymerisation. In a previous work (da Silva et al., 2008), the relationship between the free surfactant concentration trajectory and the final PSD was demonstrated. In parallel, controlling the concentration of monomer in the polymer particles allows us to avoid the presence of monomer droplets which might destabilize the latex (by adsorbing surfactant at their surface) and might delay particle nucleation in an unpredictable manner. Also, controlling the concentration of monomer in the polymer particles affects particle growth and therefore directly affects the PSD. For these reasons, the considered process outputs are the concentration of free surfactant in the aqueous phase available by conductimetry (inferential control) and the concentration of monomer in the reactor available by calorimetry, which are both easier to measure online than the PSD. Two control variables are manipulated in the proposed strategy: the surfactant and monomer flow rates. Note however that the two control actions could be decoupled and therefore two single input/single output controllers could also be developed. Decoupling would however not be perfect and therefore we prefer integrating both actions in a MIMO controller. A 2-step inferential control strategy is then developed to get the final target bimodal PSD:

Step 1) Based on a target bimodal PSD and the process model, the theoretical trajectory of concentration of free surfactant into water to follow during the reaction is calculated offline by optimization.

Step 2) This obtained theoretical trajectory of free surfactant concentration is then used in one of the two control objectives: a trajectory tracking problem is defined to control the

concentration of surfactant in the aqueous phase and is combined to a constrained set-point regulation problem of the concentration of monomer in the polymer particles (which aims at maximising the monomer concentration but avoiding the presence of droplets). The online measurements are the free surfactant concentration (by conductimetry) and the concentration of monomer (by calorimetry). The flow rates of surfactant and monomer are both manipulated online by a MIMO model-based predictive controller and are constrained in magnitude. We compare the behaviour of linearized MPC and nonlinear MPC in two simulation cases: the first case assumes a perfect model, which allows validating the methodology. The second case assumes parameter uncertainties that have important impact on the open-loop results. This test allows evaluating the performance of the controller and robustness to modelling errors.

The paper is organized as follow: first, the bulk-like model and the various balances needed are reminded. Secondly, the offline determination of the surfactant concentration is presented. Then, the linearized MPC strategy employed is reminded and applied to the described problem. Simulation results for the 2-step inferential closed-loop control approach are then discussed, in term of trajectory tracking and final PSD, both in the ideal case and with parameter uncertainties.

2 Process model

Modelling of emulsion polymerization processes leads to complex models describing different physico-chemical phenomena. The population balance of particles is important to describe particle nucleation, growth and coagulation if necessary. Material balances of the different components (initiator, radicals, monomer and surfactant) must be considered in the continuous and dispersed phase. In the following, the main model equations are given, whereas the remaining equations are given in the appendix[1].

2.1 Population balance equations

The particle size distribution during emulsion polymerizations may be described either by the pseudo-bulk model or the zero-one model. These models are combined to the reaction kinetics (propagation, terminations, transfer, and coagulation) to predict the evolution of the PSD. The pseudo-bulk model (see for instance Immanuel and Doyle III (2003)) has a general form and is available for almost all particle sizes during most of the reaction stages since it has no assumption on the number of radicals in the particles. The zero-one model (Gilbert, 1995) is adapted only for systems where the number of radicals per particle can be either 0 or 1, such as styrene polymerization and is applicable at the beginning of most reactions where the gel effect is negligible. It distinguishes: particles that have one radical, particles that have no radicals, and particles that have an oligomeric radical. Only particles containing an oligomeric radical are subject to radical desorption in this model. Edouard et al. (2005) have proposed a new representation of the zero-one model, called bulk-like model. The interest of this model is that it describes the number of particles of a specific size independently of the number of radicals they contain (which is measurable), whereas in the zero-one model, the online measurement is only a combination of the 3 states. The bulk-like model is described as:

$$\begin{cases} \dfrac{\partial n(r,t)}{\partial t} = -\dfrac{\partial}{\partial r}\left(G(r,t)\bar{n}(r,t)n(r,t)\right) \\ \dfrac{\partial \bar{n}(r,t)}{\partial t} = \rho(r,t)(1-2\bar{n}(r,t)) + \dfrac{\partial}{\partial r}\left(G(r,t)\bar{n}(r,t)n(r,t)\right)\left(\dfrac{\bar{n}(r,t)-1}{n(r,t)}\right) \\ \qquad\qquad + k_{des}(r,t)\left(\dfrac{\rho_{em}(r,t)(\bar{n}(r,t)-1)}{\rho(r,t)+[M]_p(t)(k_{pe}+k_{tr})+k_{des}(r,t)} - \dfrac{k_{tr}[M]_p(t)\bar{n}(r,t)}{\rho(r,t)+[M]_p(t)(k_{pe}+k_{tr})+k_{des}(r,t)}\right) \end{cases} \quad (1.)$$

$$\forall (r,t) \in \left[r_{nuc} \quad r_{\max}\right] \times \left]0 \quad t_f\right]$$

where $n(r,t)$ and $\bar{n}(r,t)$ are respectively the number of moles of particles and the average number of radicals in particles of size r at time t, with the following boundary conditions:

$$\begin{cases} n(r_{nuc},t) = \dfrac{\Re_{nuc}(t)}{G(r_{nuc},t)}, & \forall t > 0 \\ \overline{n}(r_{nuc},t) = 1, & \forall t > 0 \end{cases} \quad (2.)$$

and the associated initial conditions:

$$\begin{cases} n(r,0) = 0, & \forall r \in \left[r_{nuc} \quad r_{\max} \right] \\ \overline{n}(r,0) = 1, & \forall r \in \left[r_{nuc} \quad r_{\max} \right] \end{cases} \quad (3.)$$

The total nucleation rate is $\Re_{nuc}(t) = \Re_{\hom}(t) + \Re_{mic}(t)$, where the homogeneous ($\Re_{\hom}(t)$) and micellar ($\Re_{mic}(t)$) nucleation rates are given by:

$$\begin{aligned} \Re_{\hom}(t) &= k^{w}_{p_{j_{crit}-1}} [M]_w(t)[IM_{j_{crit}-1}](t)V_w \\ \Re_{mic}(t) &= \sum_{i=1}^{j_{crit}-1} k_{em,i}[Mic](t)[IM_i](t)V_w \end{aligned} \quad (4.)$$

The nucleation control variables (allowing obtaining a bimodal PSD) can be detected from the micellar nucleation rate in equation (4.). They are the concentration of micelles (determined by the concentration of surfactant into water) and the concentration of oligoradicals (affected by the concentration of initiator and monomer into water). Temperature might also affect the propagation, solubility and entry parameters which affects the nucleation rate.

Remaining equations are given in the appendix. This bulk-like model was validated by simulation by (Edouard et al., 2005) and is used in this work combined with the material balances of initiator, radicals, monomer and surfactant in order to control the PSD.

2.2 Initiator and radicals material balances in the aqueous phase

In order to calculate the concentration of radicals in the polymer particles, the material balances of radicals in the aqueous phase should be studied. As shown in table 1, the reaction is initiated in water with the initiator decomposition (*[I](t)*) that produces primary radicals

($[I^{\bullet}](t)$) that react with the monomer molecules dissolved in water to generate oligomeric radicals ($[IM_i](t)$). The total concentration of radicals in the aqueous phase ($[T](t)$) is given by:

$$[T](t) = [E](t) + [I^{\bullet}](t) + \sum_{i=1}^{j_{crit}-1} [IM_i](t) \tag{5.}$$

where $[E](t)$ is the concentration of monomeric radicals that have a lipophilic nature and can easily diffuse into and out of particles. The material balances of initiator and radicals in the aqueous phase resulting from the reactions described in table 1 are given by:

$$\frac{1}{V_w}\frac{(d[I]V_w)}{dt} = -k_d^w[I]$$

$$\frac{1}{V_w}\frac{(d[I^{\bullet}]V_w)}{dt} = 2\, f\, k_d^w[I] - (k_{pI}^w[M]_w + k_t^w[T])[I^{\bullet}]$$

$$\frac{1}{V_w}\frac{(d[IM_1]V_w)}{dt} = k_{pI}^w[M]_w[I^{\bullet}] - (k_{p1}^w[M]_w + k_t^w[T] + k_{tr}^w[M]_w)[IM_1]$$

$$\vdots$$

$$\frac{1}{V_w}\frac{(d[IM_i]V_w)}{dt} = k_{pi-1}^w[M]_w[IM_{i-1}] - (k_{pi}^w[M]_w + k_t^w[T] + k_{tr}^w[M]_w)[IM_i],\quad i = 2 \rightarrow z-1 \tag{6.}$$

$$\frac{1}{V_w}\frac{(d[IM_i]V_w)}{dt} = k_{pi-1}^w[M]_w[IM_{i-1}] - (k_{pi}^w[M]_w + k_t^w[T] + k_{tr}^w[M]_w + k_{em,i}[Mic])[IM_i]$$

$$-\frac{[IM_i]}{V_w}\int_{r_{nuc}}^{\infty} k_{e,i}(r)n(r)dr,\quad i = z \rightarrow j_{crit}-1$$

$$\frac{1}{V_w}\frac{(d[E]V_w)}{dt} = \frac{1}{V_w}\int_{r_{nuc}}^{\infty} k_{des}(r)\frac{\rho_{em}n(r)(1-\bar{n}(r)) + k_{tr}[M]_p\bar{n}(r)n(r)}{\rho(r) + [M]_p(k_{pe}+k_{tr}) + k_{des}(r)}dr$$

$$+k_{tr}^w[M]_w[T] - \frac{1}{V_w}\int_{r_{nuc}}^{\infty} k_{e,E}(r)n(r)[E]dr - k_t^w[E][T]$$

2.3 Monomer material balance

The number of moles of residual monomer is given by the material balance of monomer:

$$\frac{dN_m(t)}{dt} = Q_m(t) - k_P[M]_p(t)\frac{\bar{n}(t)N_P^T(t)}{N_A} \qquad (7.)$$

where:

- $Q_m(t)$ is the flow rate of monomer (used as a control action in our control strategy).
- The concentration of monomer in the polymer particles $[M]_p(t)$ is calculated using the partitioning coefficients considering that the monomer is partitioned between water, droplets and particles:

$$[M]_p(t) = [M]_w(t) \times k_{p-w} \qquad (8.)$$

where $[M]_w(t)$ is the concentration of monomer in the aqueous phase which is limited by the saturation value of water with monomer (interval II under saturation, and interval III bellow saturation) as follows:

$$[M]_w(t) = \begin{cases} \frac{d_m}{k_{d-w}MW_m} = [M]_w^{sat}, & \text{under saturation} \\ \frac{N_m(t)}{V_w + k_{p-w}V_p\ (t)}, & \text{else} \end{cases} \qquad (9.)$$

2.4 Surfactant material balance

The number of moles of surfactant in the reactor $N_s(t)$ is given by:

$$\frac{dN_s(t)}{dt} = Q_s(t) \qquad (10.)$$

where $Q_s(t)$ is the flow rate of surfactant (used as a control action in our control strategy). The concentration of surfactant $[S]_w(t)$ in the aqueous phase is the following:

$$[S]_w(t)V_w = N_s(t) - N_s^P(t) - N_s^d(t) \qquad (11.)$$

The concentration of micelles $[Mic](t)$ is calculated from $[S]_w(t)$ using the following expression:

$$[Mic](t) = \max\left(0, \frac{[S]_w(t) - CMC}{n_{agg}}\right) \tag{12.}$$

where *CMC* represents the critical micellar concentration of surfactant and n_{agg} is the aggregation number of surfactant in forming micelles.

2.5 Summary for the process model

The nonlinear PDE model (1-12) takes the following general form:

$$(S_{NL})\begin{cases} \dfrac{\partial x_m(\zeta,t)}{\partial t} = F_d(x_m(\zeta,t), u(t)) \ , \forall(\zeta \in \Omega, \ t > 0) \\ F_b(x_m(\zeta,t)) = 0 \ , \forall(\zeta \in \partial\Omega, \ t > 0) \\ x_m(\zeta,0) = x_m^0 \ , \forall(\zeta \in \partial\Omega \cup \Omega, \ t = 0) \\ y_m(t) = H(x_m(\zeta,t)) \ , \forall(\zeta \in \partial\Omega \cup \Omega, \ t > 0) \end{cases} \tag{13.}$$

where $x_m(\zeta,t) = [n(\zeta,t) \ \bar{n}(\zeta,t) \ [I](t) \ [I^\bullet](t) \ [IM_i](t) \ [E](t) \ N_m(t) \ N_s(t)]^T$ is the state vector, $y_m(t) = [[S]_w(t) \ [M]_p(t)]^T$ is the vector of measured and controlled outputs, $u(t) = [Q_s(t) \ Q_m(t)]^T$ is the manipulated input vector. ζ is the space variable inside the space domain Ω (with the boundary $\partial\Omega$), t is time. F_d, F_b, H are operators of suitable dimensions.

3 Offline determination of surfactant profile

As described by the process model, the surfactant is partitioned between the surface of particles, droplets (slightly) and the aqueous phase. When the concentration of surfactant in the aqueous phase exceeds the CMC, micelles are formed. If the concentration of radicals in the aqueous phase is sufficient, micelles are rapidly nucleated to form polymer particles. Therefore, the free surfactant concentration can be considered as a direct control variable of the PSD (da Silva et al., 2008).

Crowley et al. (2000) used a sequential quadratic programming method to calculate the optimal flow rate of surfactant that gives the desired PSD. Immanuel and Doyle III (2002)

used a genetic algorithm to obtain the global optimum that can then be improved using local optimization. Such algorithms are stochastic and iteratively use random processes. The choice of tuning parameters involved in genetic algorithms, such as cross-over and muting probabilities is quite difficult.

In this work, a deterministic optimization method is used. The optimization procedure aims to find the desired trajectory of free surfactant concentration ($[S]_{wref}$) that leads to the target PSD in view of the given initial conditions. This concentration is to be tracked in the online control step by comparison to the available process output (see figure 2). In order to do so, the optimisation seeks the sequence of values of surfactant flow rate that is constrained in magnitude (upper bound and lower bound).

The simulation time is 420 min and is divided into 12 intervals of 35 min each. It was found that dividing the time intervals into more than 12 intervals does not change fundamentally the optimal concentration (i.e., the final PSD tracking is no more strongly improved), whereas less than 12 intervals does not permit to solve correctly the problem (i.e., the optimization problem is not well-posed leading to large errors in the determination of the nucleation time). The PDE model (13.) used in this optimization task is first transformed into an ODE model by the finite difference method, and then solved by an ODE matlab solver. The function *lsqnonlin* in the Matlab® optimization toolbox is used to minimize the Euclidean norm between the desired and simulated PSD. A bimodal PSD, which is close to the prescribed target PSD, is obtained, as shown by figure 3. It can be seen that particle nucleation takes place as soon as the concentration of free surfactant exceeds the CMC, initially during the fifteen first minutes, due to the initial surfactant concentration and after 325 minutes due to the optimised surfactant flow rate.

Note that when nucleation is not desired, the optimisation results are not unique (the concentration of free surfactant can take any value between 0 and slightly less than the CMC).

But, in order to provoke the second nucleation, the concentration of free surfactant should exceed the CMC and therefore the same amount of surfactant is added sooner or later (e.g. the total amount of surfactant into water should increase from 0 or slightly less than the CMC to the desired amplitude above the CMC).

Note that the obtained solution remains optimal even if there is a change in the surface of particles and droplets (due for instance to a change in the monomer flow rate, reaction rate ...). Moreover, it is robust to a number of parameters due to the availability of the measurement of $[S]_w$. The only parameters that are required precisely are the CMC and n_{agg}, which are known for many surfactants.

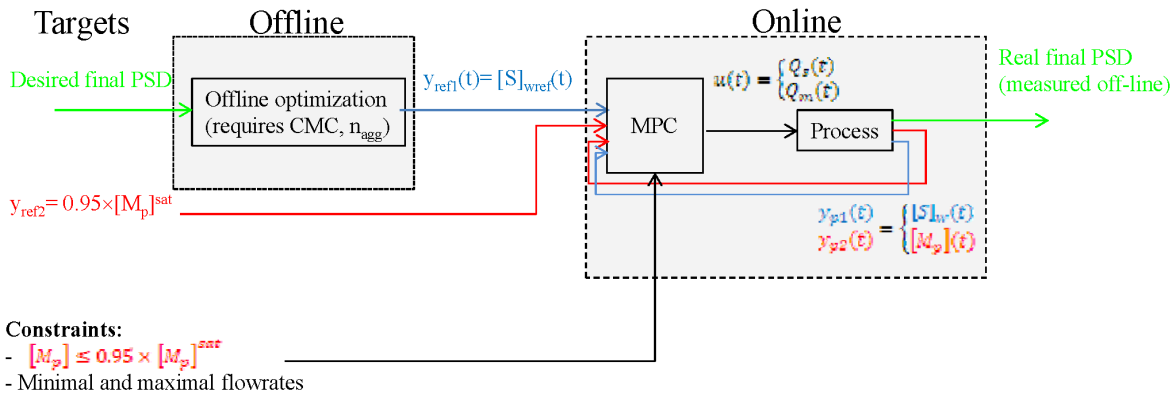

Figure 2: Offline and online optimization scheme.

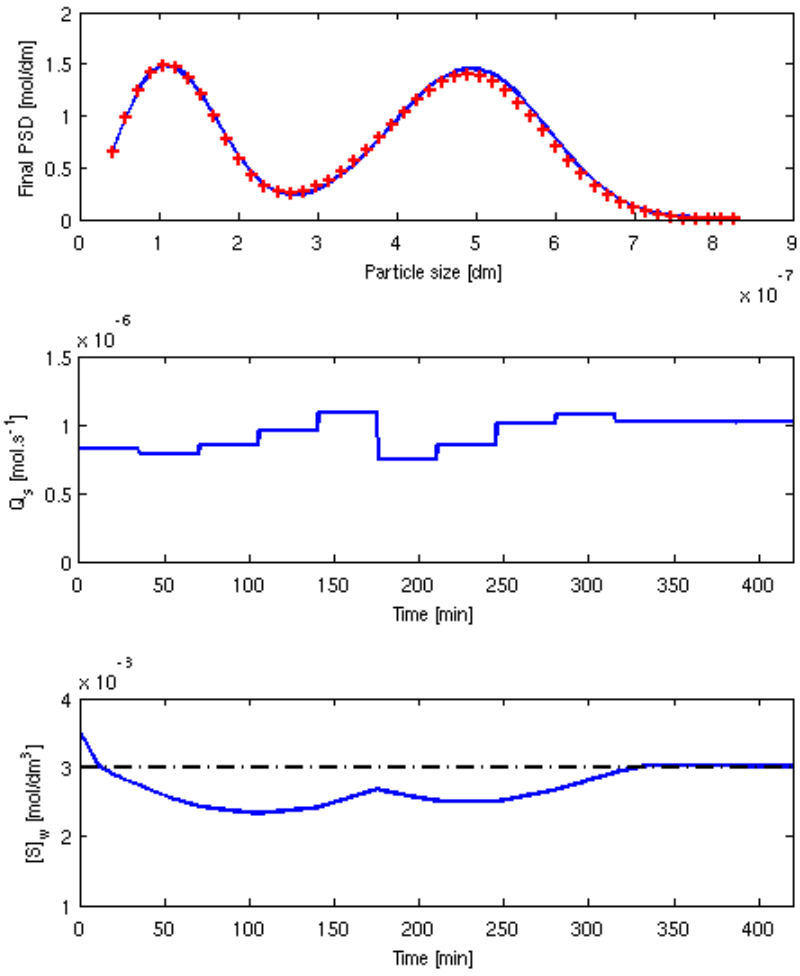

Figure 3 - Offline optimization: PSD (top +: target, top continuous: optimal solution found), optimal surfactant input flow rate found (middle) and optimal free surfactant concentration found (bottom continuous) with CMC (bottom dash-dot).

4 MPC control approach

4.1 Linearized MPC

Among the finite dimensional controllers, model predictive control is one of the most popular (Qin and Badgwell, 2003). It is a particular class of optimal control. Thousands of industrial

applications of MPC exist today, for example in the chemical and petrochemical industries. The main advantage is that constraints (due to: manipulated variables, physical limitations, operating procedures or safety reasons…) may be explicitly specified into the problem formulation. The second advantage of MPC is its ability to address long time delays, inverse responses, significant nonlinearities and multivariable interactions.

If the model exhibits a nonlinear behaviour, a numerical solution technique must be used to solve this optimization problem which leads to high computational effort. The computation effort may however be greatly reduced by linearizing the system in some manner and subsequently employing the optimisation techniques developed for linear systems (Zheng, 1997, 1998). Nevistic (1997) showed excellent simulation results when a linear time varying (LTV) system approximation was used, which was calculated at each time step over the predicted system trajectory.

A time-varying linearized PDE model-based predictive control algorithm is used in this work (for more details see Dufour et al., 2003). For pasta drying process (De Temmerman et al., 2009), the performances using this controller or a nonlinear PDE model-based controller were quite similar. However, while the nonlinear approach was not implementable (due to the short sampling time), the linearized model-based control approach was implementable. The computational time was indeed decreased by a factor 5 in the linearized case

The main idea of this approach is to transform the initial PDE constrained problem into an ODE unconstrained problem, such that the time needed to solve the online optimization problem is less than the sampling time. In order to do so, first, we define a cost function J to minimise that reflects desired process behaviour (regulation, trajectory tracking, processing time or energy consumption). Besides this cost function, output and input constraints (related to the operating conditions, safety or quality) are formulated as inequality constraints. The output constraints are handled in the optimization problem through the penalty term $J_{ext,}$ based

on the exterior penalty method. The cost function J and the penalty term J_{ext} are then combined into the penalized unconstrained cost function J_{tot} (Fletcher, 1987), where the penalty weights are tuned classically, as described in Fletcher (1987): if one output constraint is decreasing (but still larger than 0), then its weight is increased. The advantage of such output constraints handling is that all constraints of the optimization problem do not need to be absolutely satisfied for the first iteration, which is not the case for a barrier method. Hence, any initial guess may be given for the optimization argument. In this formulation, the manipulated variable u of the process is the constrained (in magnitude and velocity if needed) optimization argument. This constrained optimization argument u is then transformed into the unconstrained optimization argument d by a simple hyperbolic transformation method (Dufour et al., 2003). The optimization argument d has to be determined at each sample time k using the process measurement (or estimation), the model prediction and the penalized unconstrained cost function $J_{tot.}$. Each component of u is assumed to be a scalar (i.e. a step function over the horizon).

Then, we proceed to the linearization in order to reduce the computational time needed for the online resolution task. An offline linearization method (for more details see Dufour et al., 2003) of the nonlinear PDE model (S_{NL}) around a similar nonlinear PDE model (computed offline) (S_0) is used to formulate offline the time varying linearized PDE model (S_{TVL}). Then, online, the resolution of the time varying linearized PDE model (S_{TVL}) replaces the resolution of the nonlinear model (S_{NL}).

The last step is to approximate the PDE models by ODE models in order to be numerically solved. The control objective is then to find online the variation Δd (hence Δu) of the variable d (hence the manipulated variable u) around a chosen trajectory d_0 (hence u_0) that improves at each sample time the online optimization result, based on the model response. The final internal model structure with MPC (IMC-MPC) structure is given in figure 4.

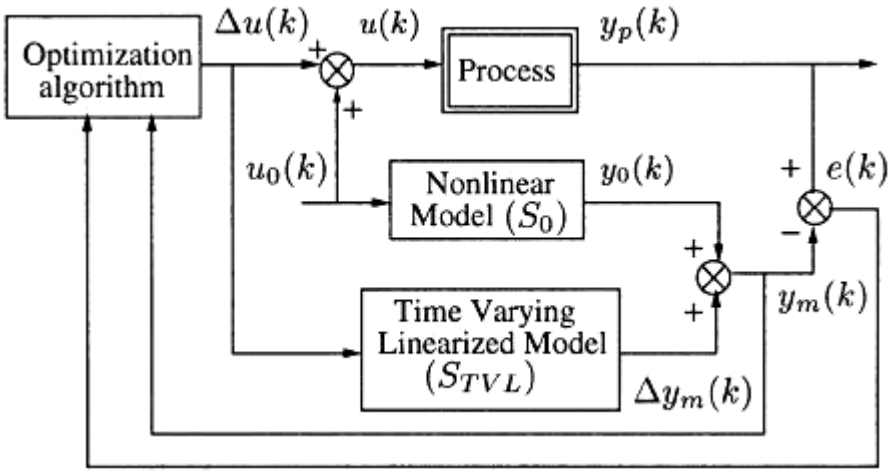

Figure 4 - General linearized IMC-MPC structure (Dufour et al., 2003).

At each current sampling instant *k* (*k* is the actual discrete index of the model and T_s is the plant sampling time, $t=k*T_s$), the proposed MPC strategy makes therefore the following actions:

- the plant measurements are collected for use in the control loop;
- the linearized plant model (S_{TVL}) is solved online to predict the output behaviour to a hypothetical set of future control sequence over a receding horizon of length *Np*.
- the unconstrained cost function J_{tot} is optimised (using a modified Levenber-Marquard algorithm). This cost function accounts for the future deviations of the predicted behaviour (from a reference behaviour) and the input-output constraints.
- the optimisation result gives a sequence of the unconstrained optimization argument *d*. The real input *u* is then calculated from *d*. Then the first value of the optimal control sequence is applied on the process.

These operations are repeated at time *k+1*. This algorithm was implemented in the MPC@CB software[2], which is used in this work.

4.2 Formulation for the PSD control

A MIMO control problem is solved here. For the first trajectory tracking problem, the reference trajectory for the free surfactant concentration ($[S]_{wref}$) is the trajectory calculate in section 3 by offline optimization. The second control objective is to maximise the monomer concentration $[M]_p$ but to maintain it below 95% of the saturation value ($[M]_p^{sat}$). Indeed, controlling the monomer concentration allows both limiting the presence of droplets and maximising the rate of particle growth (affecting therefore the PSD). Exceeding $[M]_p^{sat}$ might have detrimental effects on the control strategy of the PSD: it destabilises the particles and causes coagulation. It is obvious that a PID controller would not be able to maximise $[M]_p$ in a regulation problem and at the same time maintain it always below the defined set point: the controlled output might oscillate around it, which is not allowed here. The MIMO MPC control objective is therefore to obtain the desired $[S]_w$ as close as possible to $[S]_{wref}$ and to maintain the concentration of monomer $[M]_p$ in the polymer particles as close as possible and below the value ($0.95*[M]_p^{sat}$). The manipulated variables are the flow rates of surfactant and monomer that are constrained in magnitude. Note that the sequence of surfactant flow rate obtained in the offline optimization procedure is not used. Indeed, polymerization reactions can be irreproducible and sensitive to impurities, which makes computing the optimal flow rates (input) offline useless. In terms of available online measurements, as discussed before, the concentration of surfactant in the aqueous phase by conductimetry, and the concentration of monomer by calorimetry are used. The MIMO optimization problem that allows obtaining the prescribed bimodal PSD at the end of the polymerization reaction is stated in an MPC formulation as follows:

$$\min_{u=[Q_s(k)\ Q_m(k)]} J(u) = \gamma_1 J_1(u) + \gamma_2 J_2(u) \tag{14.}$$

with:

$$\begin{cases} J_i(u) = \sum_{j=k+1}^{j=k+N_{pi}} (y_{pi}(j) - y_{refi}(j))^2 \\ y_p = [y_{p1}\ y_{p2}]^T = \left[[S]_{wp}\ [M]_{pp} \right]^T \\ y_{ref} = [y_{ref1}\ y_{ref2}]^T = \left[[S]_{wref}\ [M]_{pref} \right]^T \\ [M]_{pref} = 0.95 \times [M]_p^{sat} \\ y_{p2}(k) \le y_{ref2} \\ u_{\min} = [Q_{s.\min}\ Q_{m.\min}]^T < u(k) < u_{\max} = [Q_{s.\max}\ Q_{m.\max}]^T \end{cases} \quad (15.)$$

5 Results

Two simulation cases are discussed:

- The first case assumes a perfect model, which helps to validate the method.
- The second case assumes a parameter uncertainty, which has an important impact on the open-loop results. This helps to evaluate the performance of the controller in a more realistic case.

In the first case, the proposed linearized MPC strategy is compared to a nonlinear MPC.

5.1 Numerical conditions

The following conditions are used:

- The PDE models are approximated using the finite difference method for spatial discretization. For the simulated process, 200 spatial discretization points ($\Delta r = 4 \times 10^{-9}$dm) are used (which is enough to be accurate), whereas in the model used in the MPC, 50 spatial discretization points ($\Delta r = 1.6 \times 10^{-8}$dm) are used (for faster computation).
- The sampling time T_s is 10s.
- The prediction horizons ($N_{P1} = N_{P2}$) are 10.
- For the magnitude constraints, the bounds are:

$$\begin{cases} Q_{s.\max} = 1\times10^{-5}\,\text{mol.s}^{-1} \\ Q_{s.\min} = 0\ \text{mol.s}^{-1} \\ Q_{m.\max} = 1\times10^{-3}\,\text{mol.s}^{-1} \\ Q_{m.\min} = 0\ \text{mol.s}^{-1} \end{cases} \qquad (16.)$$

- The initial conditions for the state are:

$$\begin{cases} n(r,0)=0,\ \forall\ r \in \left[r_{nuc} \quad r_{max} \right] \\ \overline{n}(r,0)=1,\quad \forall\ r \in \left[r_{nuc} \quad r_{max} \right] \\ I(0)= 1\times10^{-3}\ \text{mol/dm}^3 \\ [I^{\bullet}](0)=0\ \text{mol/dm}^3 \\ [IM_i](0)=0\ \text{mol/dm}^3 \\ [E](0)=0\ \text{mol/dm} \\ N_m(0)= 5.9\times10^{-3}\ \text{mol} \\ N_s(0)=4\times10^{-3}\text{mol} \end{cases} \qquad (17.)$$

- Runs are performed under Matlab R14 for Linux, with an AMD 64 3000+ 1.8GHz processor, with 2Go of RAM.

5.2 PSD control assuming perfect process modelling

In the absence of modelling errors or measurement noise, the simulation results depicted on figure 5 show that the tracking of the concentration of surfactant and the constrained regulation for the monomer concentration are almost perfect. A slight error could however be observed at the beginning of the reaction, due to the initial gap introduced between the initial conditions in the process and the references. The effect of this gap can be seen on the position and height of the first population. The obtained PSD at the end of the reaction is bimodal with almost the desired mean diameters, polydispersities and amplitudes. The calculated monomer and surfactant flow rates are physically realisable (figure 6) since they respect the predefined magnitude constraints. Results of the linearized MPC and nonlinear MPC are therefore quiet comparable. However, the nonlinear approach requires 8 times more computational time to

find the solution than the linearized MPC. In term of objective function minimisation, it is 7% higher (less precise) in the linearized approach than the nonlinear approach. In view of the computational task and the optimization results, it can be concluded that the use of nonlinear MPC is not justified. Therefore, only the linearized MPC is used in the next simulations. It is also important to highlight that using the MPC controller remains indispensable since it allows taking into account the process constraints.

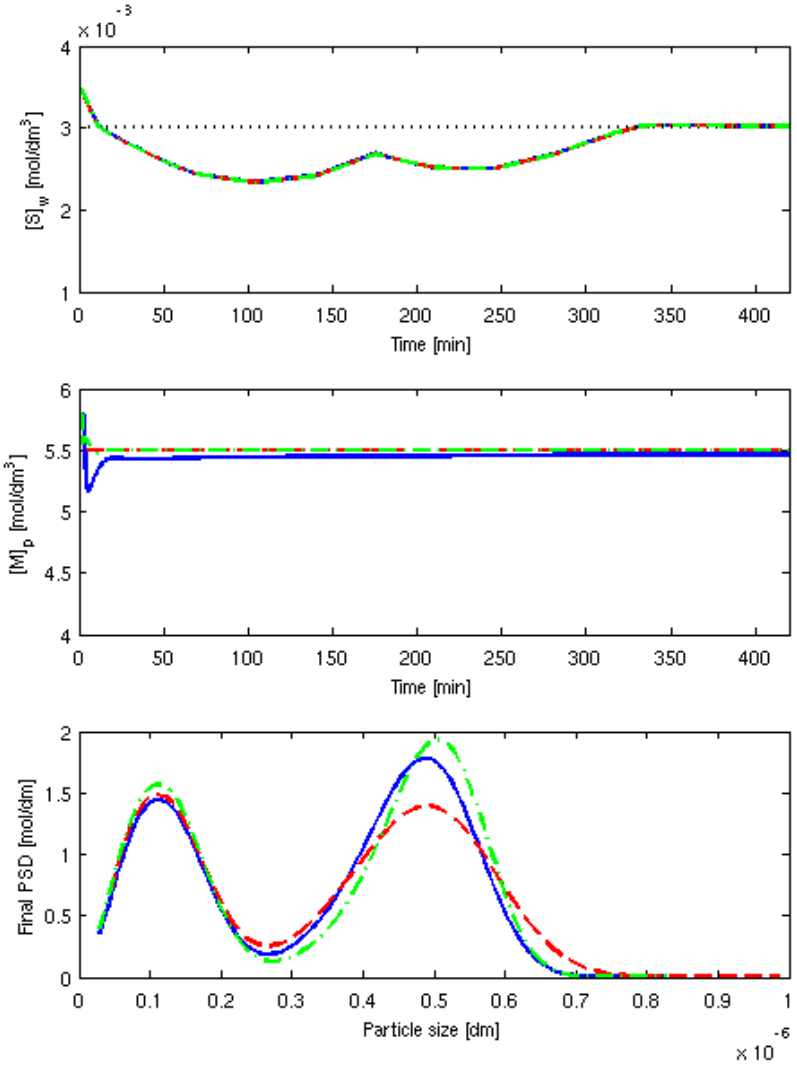

Figure 5 - Closed loop control without modeling error (target (dash), nonlinear MPC (dash dot), linearized MPC (continuous)): trajectory tracking of free surfactant concentration (top), constrained set-point tracking of monomer concentration (middle), and final PSD (bottom).

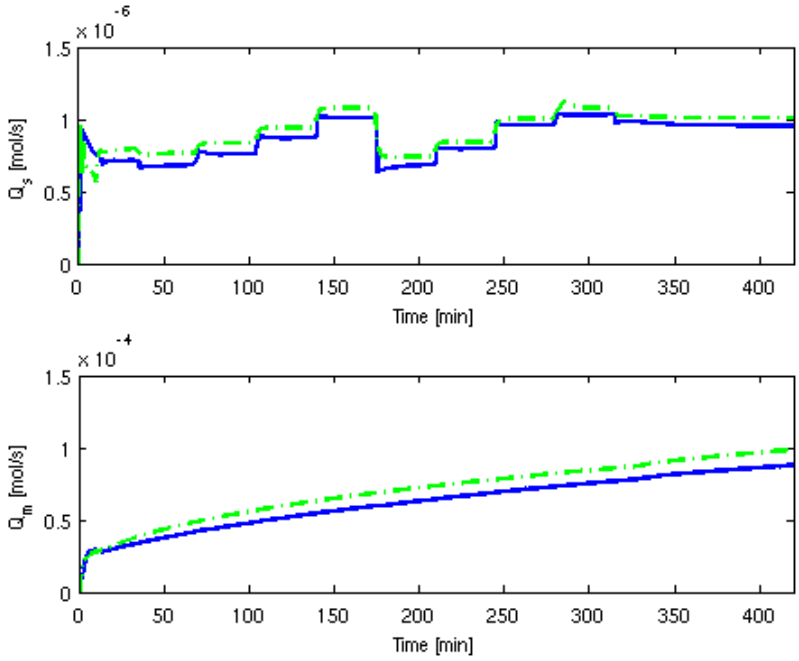

Figure 6 - Closed loop control without modeling error (nonlinear MPC (dash dot), linearized MPC (continuous)): surfactant flow rate (top) and monomer flow rate (bottom), both tuned by the controller.

5.3. PSD control with a model parameter uncertainty

A model parameter error is introduced in this section in the parameter a_{sp} which represents the particle surface that a surfactant molecule can cover. Indeed, if the surfactant contains any impurities, its efficiency to stabilise particles decreases. Furthermore, during surfactant storage, aggregation of surfactant molecules might occur which directly affects a_{sp}. In a first run, 10% of error is introduced in this parameter and in a second run it is increased to 50%. The impact of this uncertainty over the concentration of free surfactant in the aqueous phase and the monomer concentration can be seen on figures 7 and 8. In this simulation, the linearized MPC is used and is compared to open-loop model simulation (that does not use online measurements). As expected, for the open-loop model response, the calculated

concentration of free surfactant is strongly affected by the a_{sp} error (at the end of the run, the concentration of free surfactant is 50% lower compared to the case without error). Indeed, if the used value of a_{sp} is higher than its real value, the particles would adsorb more surfactant than predicted which reduces the amount of free surfactant. The calculated concentration of monomer is on the contrary almost not affected by this error (at the end of the run, the $[M]_P$ is 2.5% higher compared to the case without error) which is not surprising since there is no direct relation between a_{sp} and $[M]_P$. Due to the use of online measurements in a closed-loop manner, the optimisation task is found to lead to efficient tracking results in both output variables which leads to the desired PSD while with 50% error in a_{sp}, the obtained PSD with the open-loop model is monomodal. Indeed, in this case, the concentration of free surfactant does not exceed the CMC a second time in order to produce the second population. For the closed-loop process response, the final obtained PSD is close to the desired final shape (figure 9), especially for the second population created during the reaction, in all cases (with and without modelling error). In terms of control actions (figure 10), the surfactant flow rate is much more affected with uncertainties (up to 20%) than the monomer flow rate is (almost no difference) due to the impact of this uncertainty over both controlled output (up to 50% for the free surfactant concentration while ca. 3% for the monomer concentration). These results underline the robustness of the controller.

It can be concluded that synthesizing an optimal open-loop controller assuming perfect modelling would lead to important errors between the real and the desired PSDs, due to impurities, changes in the raw materials or due to degradation of the process components. Meanwhile, the closed-loop MIMO linearized MPC strategy is a much better strategy than open-loop policy since it reduces the impact of this error, even with high important modelling errors.

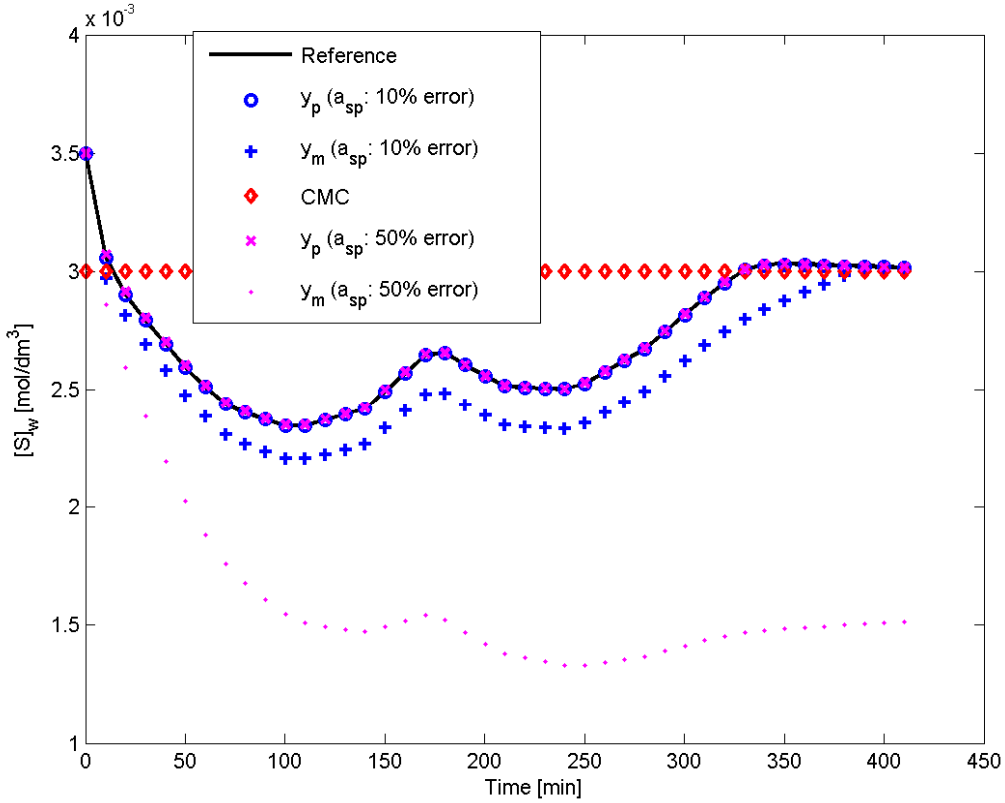

Figure 7 - Linearized MPC with parameter uncertainty: the model response y_m and the trajectory tracking for the process output y_p, both for the free surfactant concentration.

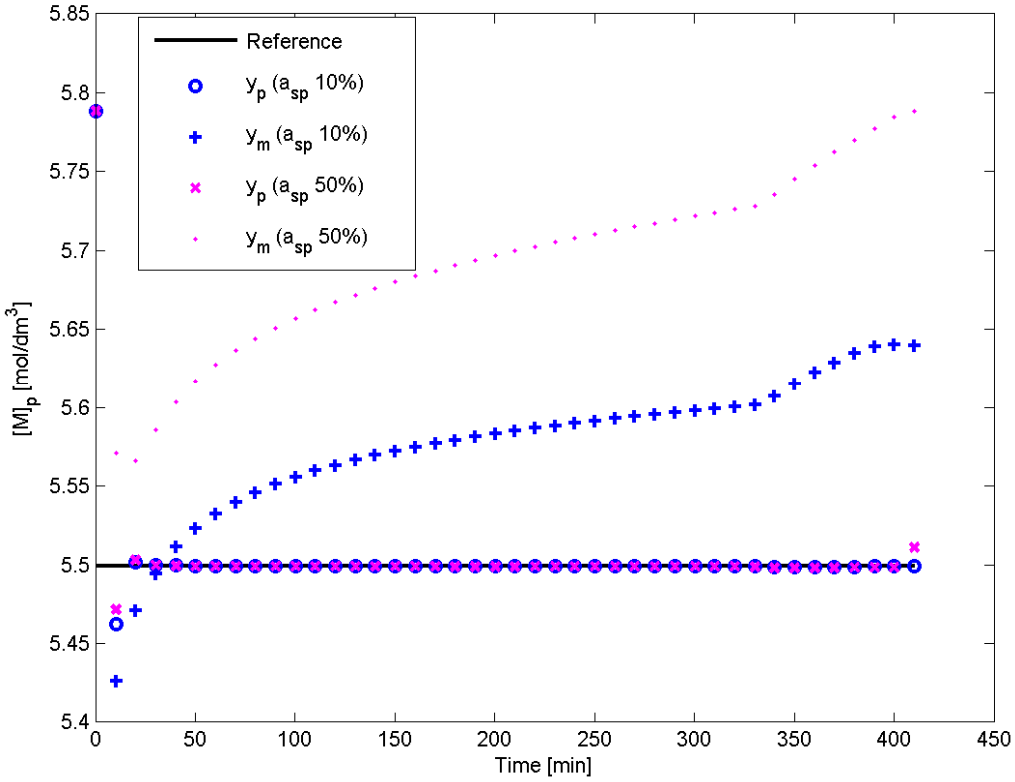

Figure 8 - Linearized MPC with parameter uncertainty: the model response y_m and the constrained set-point tracking for the process output y_p, both for the monomer concentration.

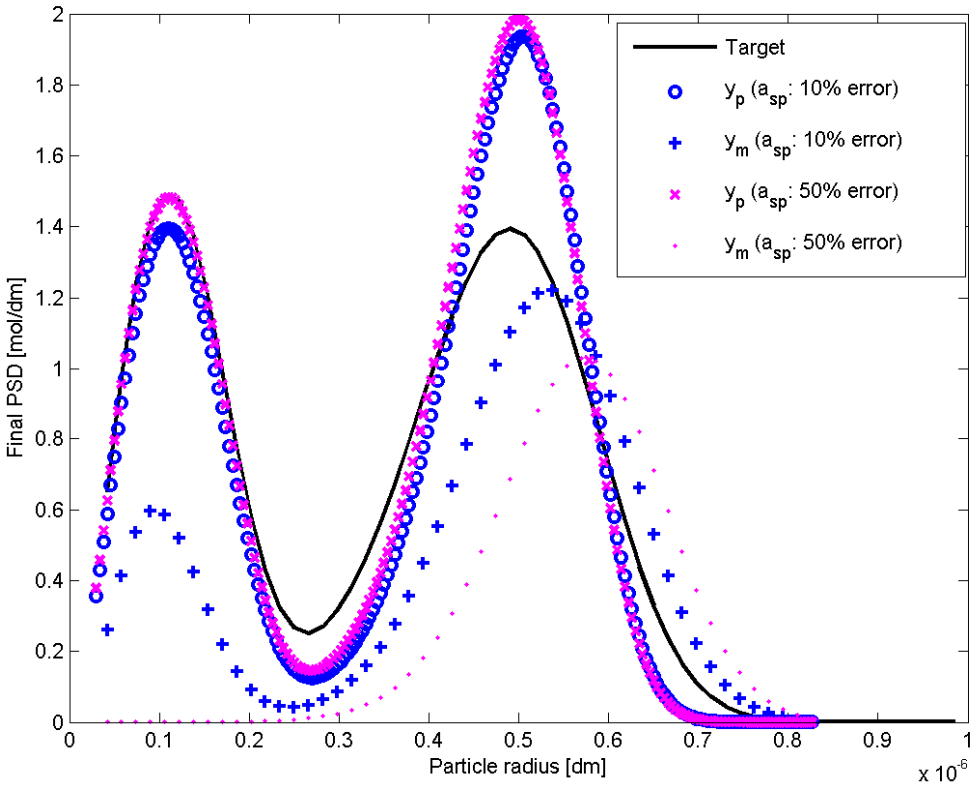

Figure 9 – Linearized MPC with parameter uncertainty: the model response y_m and the process output y_p, both in terms of final PSD.

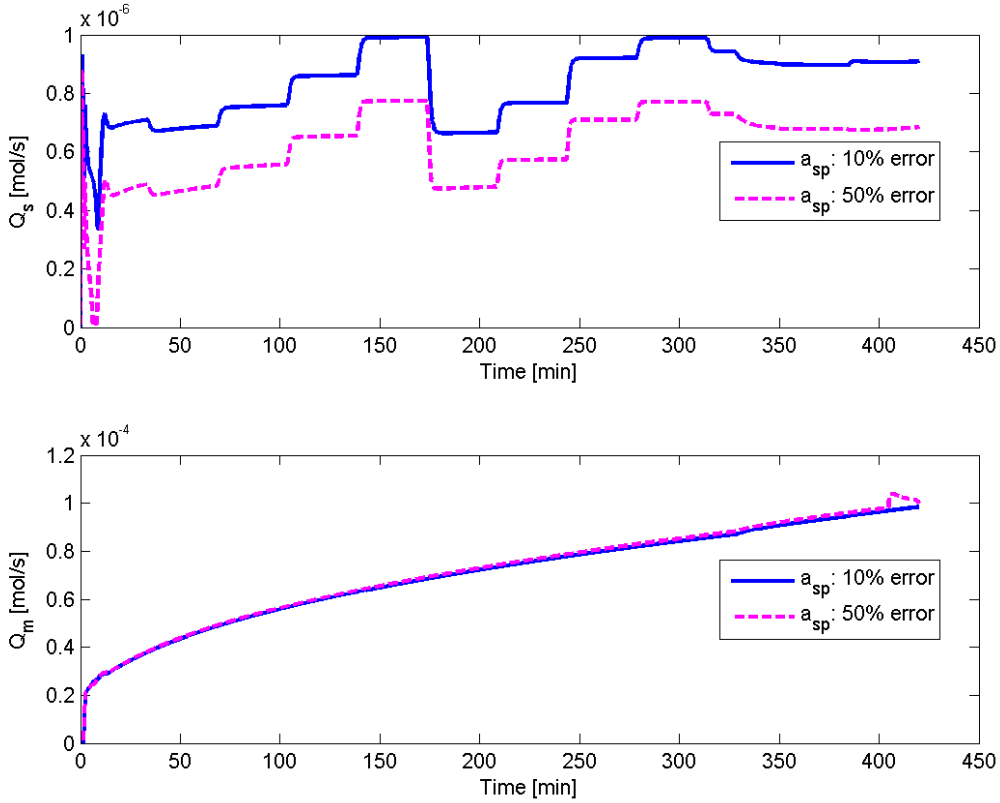

Figure 10 - Linearized MPC with parameter uncertainty: the surfactant flow rate (top) and monomer flow rate (bottom) tuned by the controller.

6. Conclusion

In this work, a new inferential model-based control strategy of the PSD in emulsion polymerisation was developed. Two online measurements were considered for the control purpose: the monomer conversion by calorimetry and the concentration of surfactant in the aqueous phase by conductimetry. The first limitation may be that conductimetry was validated experimentally only on low solid content systems. The conductimetry still can be applied to high solid content systems if a circulating and dilution loop is added. Meanwhile, it should be reminded that direct online measurement of the PSD is not available and therefore, the conductimetry represents a good alternative. Moreover, the sensors measuring the PSD are much more expensive than a simple conductimeter. This dissuades their installation for online

monitoring in the industry, even though it might be possible with a circulation loop. It is to be noted that the papers treating direct control of the PSD (based on online measurement of the PSD) were mainly simulation studies.

Here, a new 2 step MIMO control strategy for emulsion polymerisation control using MPC was constructed as follows. In the first step, the free surfactant concentration trajectory was pre-calculated offline, by model-based optimization, in order to get a predefined bimodal PSD. In the second step, a MIMO MPC was applied online to track the pre-calculated trajectory of free surfactant concentration and also to maximize the concentration of monomer in the polymer particles by a constrained set-point tracking near the saturation value. Both monomer and surfactant flow rates were manipulated online. Being model-based, the strategy is however dependent on the model quality. For example, the CMC of the surfactant should be known. This parameter is however usually well known and it evolves slightly with time during the surfactant storage. The controller strategy was validated in presence of important model parameter uncertainties (the particle surface covered by a surfactant molecule). The obtained PSD was closed to the prescribed PSD using the proposed closed-loop MPC but not using the open-loop model response.

The comparison between the linearized and nonlinear MPC strategies showed that the linearized model approach helps to decrease the calculation time by a factor of 8 while the performance degradation is lower than 7%. The linearized approach could therefore be implemented with a short sampling time (*10s*), which was not the case for the nonlinear controller. Moreover, optimization using a nonlinear model is not always evident and might not converge correctly. It should be noted however that the development time of a control strategy based on the nonlinear is more straightforward compared to the strategy based on the linearized model.

References

Abedini H, Shahrokhi M. Inferential closed-loop control of particle size distribution for styrene emulsion polymerization. Chem. Eng. Sci. 2008;63:2378-2390.

Alamir M, Sheibat-Othman N, Othman S. Measurement based modeling and control of bimodal particle size distribution in batch emulsion polymerization. AIChE J. 2010;56(8): 2122–2136.

Alhamad B, Romagnoli JA, Gomes VG. On-line multi-variable predictive control of molar mass and particle size distributions in free-radical emulsion copolymerization. Chem. Eng. Sci. 2005;60(23):6596-6606.

Berend K, Richtering W. Rheology and diffusion of concentrated monodisperse and bidisperse polymer latices. Colloids Surf., A 1995; 99:101-119.

Crowley T, Meadows E, Kostoulas E Doyle III FJ. Control of particle size distribution described by a population balance of semibatch emulsion polymerization. J. Process Control 2000;10: 419-432.

Da Silva B, Dufour P, Sheibat-Othman N, Othman S. Model predictive control of surfactant in emulsion polymerization. In proceedings of the 17th IFAC World Congress, Seoul, Korea, July 2008, 8375-8380.

De Temmerman J, Dufour P, Nicolaï B, Ramon H. MPC as control strategy for pasta drying processes. Comput. Chem. Eng. 2009;33(1), 50-57.

Dokucu MT, Doyle III, FJ. Batch-to-batch control of characteristic points on the PSD in experimental emulsion polymerization. AIChE J. 2008;54(12):3171-3187.

Dokucu MT, Park MJ, Doyle III FJ. Multi-rate model predictive control of particle size distribution in a semibatch emulsion copolymerization reactor. J. Process Control 2008;18(1):105-120.

Doyle III FJ, Harrison C, Crowley T. Hybrid model-based approach to batch-to-batch control of particle size distribution in emulsion polymerization. Comput. Chem. Eng. 2003;7:1153-1163.

Dufour P, Touré Y, Blanc D, Laurent P. On non-linear distributed parameter model predictive control strategy: On-line calculation time reduction and application to an experimental drying process. Comput. Chem. Eng. 2003;27(11):1533-1542.

Edouard D, Sheibat-Othman N, Hammouri H. Observer design for particle size distribution in emulsion polymerisation. AIChE J. 2005;51(12):3167-3185.

Elizalde O, Leal G, Leiza J. Particle size distribution measurements of polymeric dispersions: A comparative study. . Part. & Part. Syst. Charact. 2000;17:236-243.

Fletcher R. Practical methods of optimization. John Wiley and Sons, 1987.

Flores-Cerillo J, MacGregor JF. Control of particle size distributions in emulsion semibatch polymerization using mid-course correction policies. Ind. Eng. Chem. Res. 2002;41:1805-1814.

Geurts J, Lammers M, German A. The effect of bimodality of the particle size distribution on film formation of latices. Colloids Surf., A 1996;108:295-303.

Gilbert R. Emulsion polymerisation, a mechanistic approach. San Diego, Academic Press, 1995.

Immanuel CD, Doyle III FJ. Open-loop control of particle size distribution in semi-batch emulsion copolymerization using a genetic algorithm. Chem. Eng. Sci. 2002;57:4415-4427.

Immanuel CD, Doyle III FJ. Computationally efficient solution of population balance models incorporating nucleation, growth and coagulation: application to emulsion polymerization. Chem. Eng. Sci. 2003;58:3681-3698.

Immanuel C, Wang Y, Bianco N. Feedback controllability assessment and control of particle size distribution in emulsion polymerization. Chem. Eng. Sci. 2008;63(5):1205-1216.

Kiparissides C. Challenges in particulate polymerization reactor modeling and optimization: A population balance perspective. J. Process Control 2006;16:205–224.

Nevistic V. Constrained control of non linear systems. PhD thesis, ETH-Swiss Federal Institute of Technology, Zürich, Switzerland, 1997.

Qin SJ, Badgwell TA. A survey of industrial model predictive control technology. Control Eng. Pract. 2003;11(7):733-764.

Santos Jr. G, Martins C, Fortuny M, Santos A, Turmine M ,Graillat C, McKenna T. In-line and in situ monitoring of ionic surfactant dynamics in latex reactors using conductivity measurements and ion-selective electrodes. Ind. Eng. Chem. Res. 2007;46:1465-1474.

Schneider M, Claverie J, Graillat C, McKenna TF. High solids content emulsions. I. A study of the influence of the particle size distribution and polymer concentration on viscosity. J. Appl. Polym. Sci. 2002;84: 1878-1896.

Schneider M, McKenna T. Comparative study of methods for the measurement of particle size and size distribution of polymeric emulsions. Part. & Part. Syst. Charact. 2002;19:28-37.

Semino D, Ray WH. Control of systems described by population balance equations-II. emulsion polymerization with constrained control action. Chem. Eng. Sci. 1995;50:1825-1839.

Zeaiter J, Romagnoli JA, Gomes VG. On-line control of molar mass and particle-size distributions in emulsion polymerization. AIChE J. 2006;52:1770-1779.

Zheng A. A computationally efficient non linear model predictive control algorithm, in Proceedings of the American Control Conference, Albuquerque, NM, 1997.

Zheng A. Non linear model predictive control of the Tennessee–Eastman process, in Proceedings of the American Control Conference, Philadelphia, PA, 1998.

Appendix

Here are the remaining equations used by the nonlinear PDE model (1-12):

Population balance equations

The particle growth *G(r,t)* is given by:

$$G(r,t) = \frac{k_p [M]_p(t) MW_m}{4\pi r^2 d_p N_A} \tag{18.}$$

The overall rate of entry of radicals into particles is given by $\rho(r,t) = \rho_{er}(r,t) + \rho_{em}(r,t)$, with the rate of entry of oligomeric radicals into particles $\rho_{er}(r,t)$ and the rate of entry of monomeric radicals into particles $\rho_{em}(r,t)$ defined as:

$$\begin{cases} \rho_{er}(r,t) = k_{e,E}(r,t)[E](t) \\ \rho_{em}(r,t) = \sum_{i=z}^{i=j_{crit}-1} k_{e,i}(r,t)[IM_i](t) \end{cases} \tag{19.}$$

where the parameters governing radical absorption into particles or micelles and the absorption of monomeric radicals into particles are, respectively:

$$k_{e,E}(r,t) = 4\pi r_s(r,t) N_a D_w \tag{20.}$$

$$k_{e,i}(r,t) = r_s(r,t)\left(\frac{4\pi N_a D_w}{\sqrt{i}}\right), \qquad (z \le i \le j_{crit} - 1)$$

where $r_s(r)$ is the swollen radius of particles given by:

$$r_s(r,t) = r \times \left(\frac{d_m}{d_m - [M]_p(t) MW_m}\right)^{1/3} \tag{21.}$$

The desorption coefficient of monomeric radicals $k_{des}(r,t)$ is determined by:

$$k_{des}(r,t) = \frac{3D_w[M]_w(t)}{r_s^2(r,t)[M]_p(t)} \tag{22.}$$

The entry rate coefficient into micelles is:

$$k_{em,i} = r_{mic} \times \left(\frac{4\pi N_a D_w}{\sqrt{i}}\right), \quad (z \le i \le j_{crit} - 1) \tag{23.}$$

Monomer material balance

The volume of particles $V_p(t)$ is calculated by:

$$V_p(t) = \frac{4}{3}\pi N_A \int_{r_{nuc}}^{\infty} n(r,t) r^3 dr \tag{24.}$$

The average number of radicals in the polymer particles $\bar{n}(t)$ can be calculated as follows:

$$\bar{n}(t) = \frac{\int_{r_{nuc}}^{\infty} \bar{n}(r,t) n(r,t) dr}{\int_{r_{nuc}}^{\infty} n(r,t) dr} \tag{25.}$$

The total number of particles $N_P^T(t)$ is obtained by integrating the PSD over r:

$$N_P^T(t) = N_A \int_{r_{nuc}}^{\infty} n(r,t)dr \tag{26.}$$

Surfactant material balance

N_s^P *(t)* and N_s^d *(t)* are the number of moles of surfactant adsorbed on the polymer and droplet surfaces:

$$N_s^P(t) = \frac{S_p b_s [S]_w(t)}{a_{sp} N_A \left(1 + b_s [S]_w(t)\right)} \tag{27.}$$

$$N_s^d(t) = \frac{3V_d(t)}{a_{sd} r_d N_A} \tag{28.}$$

where $V_d(t)$ is the droplet volume and $S_p(t)$ the total particle surface given by:

$$\begin{cases} V_d(t) = (N_m(t) - [M]_w(t)V_w - [M]_p(t)V_p(t))\dfrac{MW_w}{d_m} \\ S_p(t) = 4\pi N_A \displaystyle\int_{r_{nuc}}^{\infty} n(r,t)r^2 dr \end{cases} \tag{29.}$$

Table 1: Kinetic scheme for aqueous phase reactions

Primary radical initiation	$I \xrightarrow{k_d^w} 2I^\bullet$
Polymer radical initiation	$I^\bullet + M \xrightarrow{k_{pI}^w} IM_1$
Propagation	$IM_i + M \xrightarrow{k_{pi}^w} IM_{i+1}$
Chain transfer to monomer	$IM_i + M \xrightarrow{k_{tr}^w} E + \textit{inactive oligomers}$
Termination	$IM_i + IM_j \xrightarrow{k_t^w}$ inactive oligomers
	$I^\bullet + T \xrightarrow{k_t^w}$ inactive oligomers
	$E + T \xrightarrow{k_t^w}$ inactive oligomers
Micellar nucleation	$IM_i + Mic \xrightarrow{k_{em,i}}$ new particle $\left(z \le i \le j_{crit} - 1\right)$
Homogeneous nucleation	$IM_{j_{crit}-1} + M \xrightarrow{k_{pj_{crit}-1}^w}$ new particle
Radical entry into particles	$IM_i + \text{particle}_n \xrightarrow{k_{e,i}} \text{particle}_{n+1}$
Entry of a monomeric radical into particles	$E + \text{particle}_n \xrightarrow{k_{e,E}} \text{particle}_{n+1}$
Desorption of a monomeric radical from particles	$\text{particle}_{n+1} \xrightarrow{k_{des}} E + \text{particle}_n$

Designation and values of the model parameters

Parameter	Designation	Value and unit
a_{sd}	Droplet surface covered by a surfactant molecule	4.2×10^{-17}dm²
a_{sp}	Particle surface covered by a surfactant molecule	4.2×10^{-17}dm²
b_s	Parameter of Langmuir isotherm	2.1×10^{3} dm^{3}.mol^{-1}
CMC	Critical micellar concentration	3×10^{-3}mol.dm^{-3}
d_m	Monomer density	0.878 kg.dm^{-3}
d_p	Polymer density	1.044 kg.dm^{-3}
D_w	Diffusion coefficient of monomer in water	1.5×10^{-7} dm².s^{-1}
[E] (t)	Concentration of monomeric radicals	mol.dm^{-3}
f	Initiator efficiency	1 [-]
G(r,t)	Particle growth	dm.s^{-1}
i	Index	[-]
[I](t)	Concentration of initiator	mol.dm^{-3}
$[I^{\bullet}](t)$	Concentration of primary radicals	mol.dm^{-3}
$[IM_i]$ *(t)*	Concentration of radicals of length i	mol.dm^{-3}
j_{crit}	Critical size of solubility of oligomers	5 [-]
$k_{d\text{-}w}$	Partitioning coefficient of monomer between droplets and the aqueous phase	1966 [-]
k_d^{w}	Decomposition rate coefficient of the initiator	7.4×10^{-7} s^{-1}
$k_{des}(r,t)$	Desorption coefficient of monomeric radicals	s^{-1}
$k_{e,E}(r,t)$	Entry rate coefficient of monomeric radicals into particles	dm^{3}.mol^{-1}.s^{-1}
$k_{em,i}$	Entry rate coefficient into micelles	dm^{3}.mol^{-1}.s^{-1}

$k_{e,i}(r,t)$	Entry rate coefficient of oligo radicals of length i into particles	$dm^3.mol^{-1}.s^{-1}$
k_p	Propagation rate coefficient of monomer into particles	260 $dm^3.mol^{-1}.s^{-1}$
$k_{p\text{-}w}$	Partitioning coefficient of monomer between particles and the aqueous phase	1348 [-]
k_{pI}^{w}	Propagation rate coefficient of a primary radical	2600 $dm^3.mol^{-1}.s^{-1}$
k_{p1}^{w}	Propagation rate coefficient of an oligomer of length 1	1200 $dm^3.mol^{-1}.s^{-1}$
k_{p2}^{w}	Propagation rate coefficient of an oligomer of length 2	280 $dm^3.mol^{-1}.s^{-1}$
k_{p3}^{w}	Propagation rate coefficient of an oligomer of length 3	260 $dm^3.mol^{-1}.s^{-1}$
k_{p4}^{w}	Propagation rate coefficient of an oligomer of length 4	260 $dm^3.mol^{-1}.s^{-1}$
k_{pe}	Coefficient of propagation of monomeric radical	260 $dm^3.mol^{-1}.s^{-1}$
k_{pe}^{w}	Propagation rate coefficient of monomeric radicals	260 $dm^3.mol^{-1}.s^{-1}$
k_t^{w}	Termination rate coefficient of radicals in the aqueous phase	1.6×10^{9} $dm^3.mol^{-1}.s^{-1}$
k_{tr}^{w}	Transfer rate coefficient to monomer in the aqueous phase	9.3×10^{-3} $dm^3.mol^{-1}.s^{-1}$
k_{tr}	Transfer rate coefficient to monomer into the particles	9.3×10^{-3} $dm^3.mol^{-1}.s^{-1}$
$[M]_p(t)$	Monomer concentration in particles	$mol.dm^{-3}$
$[M]_p^{sat}$	Monomer concentration in particles under saturation	$mol.dm^{-3}$
$[M]_w(t)$	Monomer concentration in water	$mol.dm^{-3}$
$[M]_w^{sat}$	Monomer concentration in water under saturation	5.3×10^{-3} $mol.dm^{-3}$
$[Mic]\ (t)$	Micelle concentration	$mol.dm^{-3}$
MW_M	Molecular weight of monomer	0.104 $kg.mol^{-1}$
n_{agg}	Agglomeration micellar number	60 [-]
$n(r,t)$	Number of moles of particles of size r at time t	$mol.dm^{-1}$
$\bar{n}(r,t)$	Average number of radicals per particle of size r at time t	[-]
$\bar{n}(t)$	Average number of radicals per particle at time t	[-]

N_A	Avogadro's number	6.022×10^{23} mol^{-1}
$N_m(t)$	Number of moles of residual monomer	mol
$N_s(t)$	Total number of moles of surfactant	mol
$N_s^P(t)$	Number of moles of surfactant on particles' surface	mol
$N_s^d(t)$	Number of moles of surfactant on droplets' surface	mol
$N_P^T(t)$	Total number of particles	[-]
$Q_m(t)$	Monomer flow rate	mol.s^{-1}
$Q_s(t)$	Surfactant flow rate	mol.s^{-1}
r	Radius	dm
r_d	Droplet radius	1.1×10^{-4} dm
r_{max}	Maximum radius considered in the PSD calculation	8.26×10^{-7} dm
r_{mic}	Micelle radius	2.6×10^{-8} dm
r_{nuc}	Nucleation radius	2.6×10^{-8} dm
$r_s(r)$	Swollen radius of particles	dm
$\Re_{\text{hom}}(t)$	Homogeneuous nucleation rate	mol.s^{-1}
$\Re_{\text{mic}}(t)$	Micellar nucleation rate	mol.s^{-1}
$\Re_{nuc}(t)$	Total nucleation rate	mol.s^{-1}
$\rho(r,t)$	Overall rate of entry of radicals into particles	mol.s^{-1}
$\rho_{er}(r,t)$	Rate of entry of oligomeric radicals into particles	mol.s^{-1}
$\rho_{em}(r,t)$	Rate of entry of monomeric radicals into particles	mol.s^{-1}
$[S]_w(t)$	Surfactant concentration in water	mol.dm^{-3}
$S_p(t)$	Total particle surface	dm^2
t	Time	s
t_f	Final time	s

[T] (t)	Total concentration of radicals in the aqueous phase	mol.dm^{-3}
$V_d(t)$	Volume of droplets	dm^3
V_p *(t)*	Volume of particles	dm^3
V_w	Volume of the aqueous phase	1 dm^3
z	Minimum number of units of monomer in the radical for particle entry	3 [-]

Notations for the control strategy

d	Unconstrained manipulated variable
d_0	Unconstrained manipulated variable for S_0
Δd	Unconstrained manipulated variable for S_{TVL}
F_b, F_d, H	Nonlinear operators
j	Discrete time index in the future
k	Actual discrete time index
J, J_1, J_2	Cost function
J_{ext}	Exterior penalty function
J_{tot}	Total penalized cost function
N_p, N_{p1}, N_{p2}	Prediction horizons (-)
S_{NL}	Nonlinear model
S_0	Nonlinear model computed off-line
S_{TVL}	Time-varying linearized model computed online
t	Time (s)
T_s	Sampling time (s)
u	Manipulated variable
u_{min}	Minimum magnitude allowed for the manipulated variable
u_{max}	Maximum magnitude allowed for the manipulated variable
u_0	Manipulated variable for S_0
Δu	Manipulated variable for S_{TVL}

x_m	Model state
y_p, y_{p1}, y_{p2}	Process output
$y_{ref}, y_{ref1}, y_{ref2}$	Reference behavior
$\partial\Omega$	Boundary of the spatial domain
Ω	Spatial domain
ζ	Space variable (m)
γ_1, γ_2	Weight for the cost functions

Table footnotes

1 The time dependence of some variables is voluntary not written, in order to have an easier reading. Theses details may be found in the table “Designation and values of the model parameters”.

2 © University Claude Bernard Lyon 1 - EZUS. In order to use MPC@CB, please contact the author: dufour@lagep.univ-lyon1.fr . Visit the website dedicated to this software: http://MPC-AT-CB.univ-lyon1.fr